

Field dynamics and kink-antikink production in rapidly expanding systems

G. Holzwarth*

Institute of Theoretical Physics, University of Stellenbosch, 7602 Matieland, South Africa

Field dynamics in a rapidly expanding system is investigated by transforming from space-time to the rapidity - proper-time frame. The proper-time dependence of different contributions to the total energy is established. For systems characterized by a finite momentum cut-off, a freeze-out time can be defined after which the field propagation in rapidity space ends and the system decays into decoupled solitons, antisolitons and local vacuum fluctuations. Numerical simulations of field evolutions on a lattice for the (1+1)-dimensional Φ^4 model illustrate the general results and show that the freeze-out time and average multiplicities of kinks (plus antikinks) produced in this 'phase transition' can be obtained from simple averages over the initial ensemble of field configurations. An extension to explicitly include additional dissipation is discussed. The validity of an adiabatic approximation for the case of an overdamped system is investigated. The (3+1)-dimensional generalization may serve as model for baryon-antibaryon production after heavy-ion collisions.

PACS numbers: 11.10.Lm, 11.27.+d, 25.75.-q, 64.60.Cn, 75.40.Mg

Keywords: Rapid expansion, topological textures, heavy-ion collisions, freeze-out

arXiv:hep-ph/0303208v2 20 May 2003

* Permanent address: Fachbereich Physik, Universität Siegen, D-57068 Siegen, Germany
e-mail: holzwarth@physik.uni-siegen.de

I. INTRODUCTION

It is a commonly accepted scenario for central ultra-relativistic heavy-ion collisions that immediately after the collision, sandwiched between the receding baryonic pancakes, a rapidly expanding spatial region is left, characterized by high energy density and low baryon density [1]. The expansion may be mainly in beam direction, such that the longitudinal velocities of volume elements are proportional to their distance from the collision point. Assuming invariance with respect to transformations between comoving frames, the rapidity density of particles emitted from this expanding rod will show a plateau reflecting that symmetry. This plateau is experimentally well established, and recent results for baryonic yields indicate that for high centrality and increasing energy the antibaryon/baryon ratio in fact tends towards unity [2, 3, 4].

The production of baryon-antibaryon pairs from regions of highly excited 'vacuum' presents a challenge for many different types of theoretical models. It arises very naturally in models where baryon density is identified with topological winding density in effective meson field theories [5, 6, 7, 8]. For random field configurations on random triangular lattices the probability for nontrivial winding provides an upper (Kibble) limit for baryon-antibaryon multiplicities [9, 10]. The dynamical evolution in time, which follows the preparation of a statistical ensemble at some initial time, tends to smoothen the random initial configurations, resulting in frequent 'annihilation' of positive and negative winding density, such that the final baryon-antibaryon multiplicities will strongly depend on the cooling mechanism and freeze-out times, after which the system is sufficiently decoupled, such that baryons and antibaryons no longer interact [11, 12, 13, 14].

Apart from genuine energy dissipation through meson emission, the rapid expansion provides a kinetic cooling mechanism which naturally decreases all gradients in a field configuration and, consequently, the winding densities. This expansion is conveniently accounted for by transforming the space-time frame into the rapidity - proper-time frame and formulating the field dynamics in these locally comoving frames [15, 16, 17, 18, 19, 20, 21]. We repeat the essential points of this formulation in section II, with specific attention to the soliton solutions. We also include the effects of genuine damping and discuss the adiabatic approximation which applies for overdamped systems and provides significant simplifications in the numerical simulation of such evolutions.

In section III of the present paper we apply this formalism to the (1+1) dimensional Φ^4 model, which is characterized by only two discrete degenerate vacua. This provides a very transparent example for the mechanisms which govern the 'phase transition' from the hot initial configurations through the freeze-out into the final cold system which has settled into the true vacua and consists of non-interacting solitons and vacuum fluctuations. We obtain simple analytical expressions for freeze-out time and kink multiplicities, both for the system moving freely in the expanding Bjorken rod, and for the damped system which additionally loses energy through a dissipative term.

II. FIELD DYNAMICS IN THE RAPIDITY - PROPER-TIME FRAME

A. Transformation to Bjorken frame

As standard effective action \mathcal{S} for a scalar field Φ in space-time (z, t) we consider

$$\mathcal{S} = \int \left(\frac{1}{2}(\partial_t \Phi)^2 - \frac{1}{2}(\partial_z \Phi)^2 - V(\Phi) \right) dz dt \quad (1)$$

where $V(\Phi)$ denotes a suitable local self-interaction. The transformation from (z, t) to proper time τ and rapidity η is defined as

$$\begin{aligned} t &= \tau \cosh \eta, & \tau &= \sqrt{t^2 - z^2}, & \partial_t &= \cosh \eta \partial_\tau - \frac{\sinh \eta}{\tau} \partial_\eta \\ z &= \tau \sinh \eta, & \eta &= \operatorname{atanh} \left(\frac{z}{t} \right), & \partial_z &= -\sinh \eta \partial_\tau + \frac{\cosh \eta}{\tau} \partial_\eta. \end{aligned} \quad (2)$$

The boundaries in the forward light cone are (note: $dz dt = \tau d\tau d\eta$)

$$\int_0^\Lambda dt \int_{-t}^t dz \implies \int_0^\Lambda \tau d\tau \int_{-\operatorname{atanh} \sqrt{1-(\tau/\Lambda)^2}}^{\operatorname{atanh} \sqrt{1-(\tau/\Lambda)^2}} d\eta. \quad (3)$$

Note that (only) for $\tau = 0$ the η -integral extends from $-\infty$ to $+\infty$. We therefore consider instead the action

$$\mathcal{S} = \int d\tau \int_{-\infty}^{+\infty} \mathcal{L} d\eta = \int (T - L_2 - U) d\tau \quad (4)$$

with

$$T(\tau) = \frac{\tau}{2} \int_{-\infty}^{+\infty} (\partial_\tau \Phi)^2 d\eta, \quad L_2(\tau) = \frac{1}{2\tau} \int_{-\infty}^{+\infty} (\partial_\eta \Phi)^2 d\eta, \quad U(\tau) = \tau \int_{-\infty}^{+\infty} V(\Phi) d\eta. \quad (5)$$

Variation with respect to Φ then leads to the equation of motion (EOM) $\delta\mathcal{S}/\delta\Phi = 0$:

$$\frac{1}{\tau} \partial_\tau \Phi + \partial_{\tau\tau} \Phi - \frac{1}{\tau^2} \partial_{\eta\eta} \Phi + \delta V/\delta\Phi = 0. \quad (6)$$

Consider the total energy $E(\tau)$ at a given proper time τ

$$E(\tau) \equiv \int ((\delta\mathcal{S}/\delta\partial_\tau \Phi) \cdot \partial_\tau \Phi - \mathcal{L}) d\eta = (T(\tau) + L_2(\tau) + U(\tau)). \quad (7)$$

The total derivative of this energy with respect to proper time τ is

$$\begin{aligned} \frac{dE}{d\tau} &= \frac{\partial E}{\partial \tau} + \int \left(\frac{\delta E}{\delta \partial_\tau \Phi} \partial_{\tau\tau} \Phi + \frac{\delta E}{\delta \Phi} \partial_\tau \Phi \right) d\eta \\ &= \frac{1}{\tau} (T - L_2 + U) + \tau \int \left(\partial_{\tau\tau} \Phi - \frac{1}{\tau^2} \partial_{\eta\eta} \Phi + \delta V/\delta\Phi \right) \partial_\tau \Phi d\eta. \end{aligned} \quad (8)$$

Using EOM (6) leads to

$$\frac{dE}{d\tau} = \frac{1}{\tau} (-T - L_2 + U) = -\frac{1}{\tau} (E - 2U). \quad (9)$$

This is solved by

$$E = \frac{C}{\tau} + \frac{2}{\tau} \int^\tau U d\tau \quad (10)$$

with constant C .

1. Two remarks:

(A): If the potential $V(\Phi)$ averaged over rapidity is independent of proper time τ (as can be realized for random distributions of Φ in rapidity space, i.e. during the early phase of an evolution) such that we have $U \propto \tau$, then a simple solution to (9) is obtained

$$T + L_2 = \frac{C_0}{\tau}, \quad \text{i.e.} \quad E = \frac{C_0}{\tau} + C_1 \tau \quad (11)$$

with constants C_0 and C_1 . The first term (solving the homogenous part of eq.(9)) looks like damping, but it is a purely geometrical decrease. (Its time integral is still divergent).

(B): If the energy for large proper times $\tau \rightarrow \infty$ approaches a finite constant $E(\tau) \rightarrow E_\infty$, then eq.(9) requires that

$$\lim_{\tau \rightarrow \infty} (T(\tau) + L_2(\tau) - U(\tau)) = 0 + \text{fluct.} \quad (12)$$

with eventual fluctuations in U and $T + L_2$ (which, however have to add up to a smooth total energy $E(\tau)$, because of $\frac{dE}{d\tau} \rightarrow 0$). For proper-time averages over at least one period of the fluctuations we have

$$\lim_{\tau \rightarrow \infty} \langle (T(\tau) + L_2(\tau)) \rangle = \lim_{\tau \rightarrow \infty} \langle U(\tau) \rangle = E_\infty/2. \quad (13)$$

(B1): This may be realized such that for large τ all time derivatives disappear ($T \rightarrow 0$) and $L_2 = U \rightarrow E_\infty/2$. This represents an ensemble of adiabatically shrinking solitons which carry all of the conserved energy E_∞ (see below).

(B2): Another way to arrive at an asymptotically constant E appears if the gradient terms L_2 become negligible after a long time. Then eq.(13) requires that asymptotically $\langle U \rangle$ and $\langle T \rangle$ are equal and constant in proper time. This implies that there exist non-vanishing average time-derivatives in the system which decrease like $1/\sqrt{\tau}$ in proper time.

B. Shrinking solitons at rest in the Bjorken frame

For a stability condition we omit all time-derivative terms, i.e. put $T = 0$ and keep in the EOM only

$$-\frac{1}{\tau^2}\partial_{\eta\eta}\Phi + \delta V/\delta\Phi = 0. \quad (14)$$

This equation describes extended objects whose size in rapidity space shrinks proportional to increasing proper time, which here simply acts as a scaling parameter. The derivative of their total energy $E = L_2 + U$ with respect to proper time is given by

$$\frac{dE}{d\tau} = \frac{1}{\tau}(U - L_2). \quad (15)$$

From multiplying EOM (12) with $\partial_\eta\Phi$ we have

$$\partial_\eta \left(-\frac{1}{2\tau^2}(\partial_\eta\Phi)^2 + V(\Phi) \right) = 0, \quad (16)$$

or, if the integrals are finite,

$$L_2 = U, \quad \text{and} \quad dE/d\tau = 0. \quad (17)$$

This result, that for the shrinking solitons L_2 and U are independent of proper time, can of course be obtained by simply replacing $\Phi(\eta)$ by $\Phi_\tau(\eta) = \Phi(\tau\eta)$ in the definitions (5).

However, this only holds in an adiabatic limit, where proper time can be considered as a parameter. In fact, for the shrinking solitons we have $\partial_\tau\Phi_\tau = (\eta/\tau)\partial_\eta\Phi_\tau$, so

$$T = \frac{1}{2\tau^2} \int \eta^2 (\partial_\eta\Phi(\eta))^2 d\eta. \quad (18)$$

So, in the limit of large proper times, T becomes rapidly negligible as compared to the constants L_2 and U , and E is asymptotically conserved.

C. Including a dissipative term

Genuine dissipation is taken into account by adding a dissipative term to the EOM. With dissipation constant γ , eq.(6) now reads

$$\left(\gamma + \frac{1}{\tau}\right)\partial_\tau\Phi + \partial_{\tau\tau}\Phi - \frac{1}{\tau^2}\partial_{\eta\eta}\Phi + \delta V/\delta\Phi = 0. \quad (19)$$

Inserting this into eq.(8) we have

$$\frac{dE}{d\tau} = -\frac{1}{\tau}(E - 2U) - \gamma\tau \int (\partial_\tau\Phi)^2 d\eta. \quad (20)$$

The first term again is purely geometrical, while the rate of energy loss due to dissipation is given by the second term alone

$$\left(\frac{dE}{d\tau}\right)_{\text{diss}} = -\gamma\tau \int (\partial_\tau\Phi)^2 d\eta. \quad (21)$$

It is equal to -2γ times the kinetic energy T , so we have

$$\frac{d(T + L_2 + U)}{d\tau} = -\frac{1}{\tau}(T + L_2 - U) - 2\gamma T. \quad (22)$$

For the early stages of an evolution, in analogy to (11), we expect for the smooth parts of T , L_2 , and U

$$\langle T + L_2 \rangle = \frac{C_0}{\tau}f(\tau), \quad \langle U \rangle = C_1\tau. \quad (23)$$

The function $f(\tau)$ satisfies the differential equation

$$\frac{df}{f} = -2\gamma \frac{\langle T \rangle}{\langle T + L_2 \rangle} d\tau. \quad (24)$$

The dissipation will exponentially reduce the kinetic gradients as compared to the rapidity gradients, so for the smooth parts $\langle T \rangle$ and $\langle L_2 \rangle$ we try the ansatz

$$\langle T \rangle = \exp(-\alpha\gamma\tau) \langle L_2 \rangle, \quad (25)$$

where we have allowed for an as yet undetermined constant α . This leads to

$$f(\tau) = \left(\frac{1 + e^{-\alpha\gamma\tau}}{1 + e^{-\alpha\gamma\tau_0}} \right)^{2/\alpha} \quad (26)$$

if we require that $f(\tau_0) = 1$ for all values of γ , i.e. if for the initial configurations at $\tau = \tau_0$ the integrals $T + L_2$ are independent of γ . This provides an analytical expression for $\langle L_2 \rangle$

$$\langle L_2 \rangle = \frac{C_0}{\tau} \frac{(1 + e^{-\alpha\gamma\tau})^{2/\alpha-1}}{(1 + e^{-\alpha\gamma\tau_0})^{2/\alpha}} \quad (27)$$

as compared to explicitly solving the EOM (19). We shall see below that its intersection with the linearly rising potential $\langle U \rangle = C_1\tau$ may be used to define a simple estimate for the freeze-out time τ_f .

D. Adiabatic Approximation

For large values of γ , such that $\gamma\tau_0 \gg 1$, all fluctuating terms are suppressed from the very beginning, the evolutions get overdamped and we may approximate the EOM (19) by omitting all second-order time derivatives. As $\tau > \tau_0$, it is then also sufficient to keep in the dissipative terms only the constant γ

$$\gamma \partial_\tau \Phi - \frac{1}{\tau^2} \partial_{\eta\eta} \Phi + \delta V / \delta \Phi = 0. \quad (28)$$

With this equation of motion we now have

$$\frac{d(L_2 + U)}{d\tau} = \frac{1}{\tau} (-L_2 + U) - 2\gamma T. \quad (29)$$

Proceeding as in equations (23) and (24), with $U = C_1\tau$, we now have

$$L_2 = \frac{C_0}{\tau} \exp\left(-2\gamma \int_{\tau_0}^{\tau} (T/L_2) d\tau\right). \quad (30)$$

With a suitable ansatz for the ratio T/L_2 during the early part of the evolution we may again obtain a simple expression for L_2 and, in connection with $U = C_1\tau$, for the freeze-out time τ_f .

III. SIMPLE EXAMPLE: Φ^4 -MODEL

The Φ^4 -model uses the local potential

$$V(\Phi) = \frac{\lambda}{4} (\Phi^2 - 1)^2, \quad (31)$$

so the action \mathcal{S} in (z, t) -coordinates is

$$\mathcal{S} = \int \left(\frac{1}{2} (\partial_t \Phi)^2 - \frac{1}{2} (\partial_z \Phi)^2 - \frac{\lambda}{4} (\Phi^2 - 1)^2 \right) dz dt. \quad (32)$$

For stable static solitons we have [22]

$$\frac{1}{2} \int (\partial_z \Phi)^2 dz = \frac{\lambda}{4} \int (\Phi^2 - 1)^2 dz = \frac{\sqrt{2\lambda}}{3}. \quad (33)$$

A. Shrinking solitons in the Bjorken frame

After transforming to the Bjorken frame the stability condition (14) looks like the equation for stable static solutions in the rest frame with λ replaced by $\lambda\tau^2$. So we have according to eq.(33)

$$\frac{1}{2} \int (\partial_\eta \Phi)^2 d\eta = \tau^2 \frac{\lambda}{4} \int (\Phi^2 - 1)^2 d\eta = \tau \frac{\sqrt{2\lambda}}{3}. \quad (34)$$

With definitions (5), we find

$$L_2 = U = E/2 = \frac{\sqrt{2\lambda}}{3} = \text{const}_\tau. \quad (35)$$

So, in the (adiabatic, i.e. $T \rightarrow 0$) limit of large proper times the total energy of the shrinking solitons in the Bjorken frame approaches a constant which coincides with their static energy in the (z, t) -frame. This represents a realization of the above remark (B1) in section II.

It should, however, be noted that on a lattice these relations are violated if with increasing proper time the shrinking size $(\tau\sqrt{\lambda/2})^{-1}$ of the stable solitons approaches the lattice constant (set equal to one). Gradients for single solitons then cannot exceed the value of 2 (corresponding to a jump in Φ from -1 to +1 for neighbouring lattice points). So we have

$$L_2 \rightarrow n \frac{2}{\tau} \quad \text{for} \quad \tau \rightarrow \infty, \quad (36)$$

where n is the final number of kinks+antikinks surviving for large proper times. This means that L_2 will not approach a constant, but will decrease like $1/\tau$, while the kinks' contribution to U rapidly goes to zero like τ^{-3} . So, on a lattice, $dE/d\tau = 0$ cannot be reached in an adiabatic limit for large proper times. Still, $dE/d\tau \rightarrow 0$ for $\tau \rightarrow \infty$ can be realized by balancing fluctuational contributions to T and U such that E is constant, which constitutes a non-adiabatic realization of the remark (B2) discussed in section II.A.

B. Evolutions on a lattice

1. Symmetric potential

Let us first consider evolutions in the symmetric potential

$$V^{(+)}(\Phi) = \frac{\lambda}{4} ((\Phi^2 + 1)^2 - 1), \quad (37)$$

which has only one single minimum at $\Phi = 0$. (We subtract the constant -1 to maintain $V(0) = 0$). So, a priori, we would not expect any 'phase transition' to occur in this potential. Initial configurations at $\tau = \tau_0 \ll 1$ for the evolutions consist of values Φ_i at each lattice point $i = 0, \dots, N$, randomly chosen from a normalized Gaussian distribution

$$f(\Phi) = \frac{1}{\sqrt{2\pi\sigma^2}} \exp\left(-\frac{\Phi^2}{2\sigma^2}\right) \quad (38)$$

with mean square deviation $\overline{\Phi^2} = \sigma^2$. So, the system looks similar for all rapidity intervals that make up the η lattice.

The integral

$$\int V^{(+)}(\Phi) d\eta \implies N \int V^{(+)}(\Phi) f(\Phi) d\Phi \quad (39)$$

for sufficiently small width $\sigma \ll 1$ is approximated by

$$N \frac{\lambda}{2} \int \Phi^2 f(\Phi) d\Phi = N \frac{\lambda}{2} \sigma^2. \quad (40)$$

So, the initial value of $U^{(+)}$ at $\tau = \tau_0$ is given by $N \frac{\lambda}{2} \sigma^2 \tau_0$, while $U^{(+)}(\tau)$ will be oscillating around the time-averaged $\langle U^{(+)} \rangle$ given by the straight line

$$\langle U^{(+)} \rangle = N \frac{\lambda}{4} \sigma^2 \tau. \quad (41)$$

For an estimate of the integral $\int (\partial_\eta \Phi)^2 d\eta$ we implement the first derivatives on the lattice as $\Phi_{i+1} - \Phi_i$ and obtain

$$\frac{1}{2} \int (\partial_\eta \Phi)^2 d\eta \implies \sum (\Phi_i)^2 - \sum \Phi_{i+1} \Phi_i = N(\bar{\Phi}^2 - \bar{\Phi}^2). \quad (42)$$

For the second equality we have assumed that the two-point correlation function $\sum \Phi_{i+1} \Phi_i$ factorizes, i.e. that Φ -values at neighbouring lattice points are uncorrelated. So, the initial value for L_2 at $\tau = \tau_0$ is given by

$$L_2(\tau_0) = N \frac{\sigma^2}{\tau_0}. \quad (43)$$

The initial values for the proper time derivatives $\partial_\tau \Phi_i(\tau_0)$ are not relevant and we can put them to zero. The equations of motion immediately after the onset of the evolution build up T such that the smooth sum $T + L_2$ closely follows the line $N\sigma^2/\tau$, while T and L_2 separately oscillate around the time averaged values

$$\langle L_2 \rangle = \langle T \rangle = N \frac{\sigma^2}{2\tau}. \quad (44)$$

During this early phase of the evolution the potential is unimportant because it is suppressed by two orders of τ as compared to L_2 . The proper time value

$$\tau_f^2 = 2/\lambda \quad (45)$$

marks the intersection of $\langle L_2 \rangle$ with the potential $\langle U^{(+)} \rangle$ where $U^{(+)}$ begins to influence the motion. This marks the end of this first (gradient-dominated) phase which consists of freely propagating fluctuations.

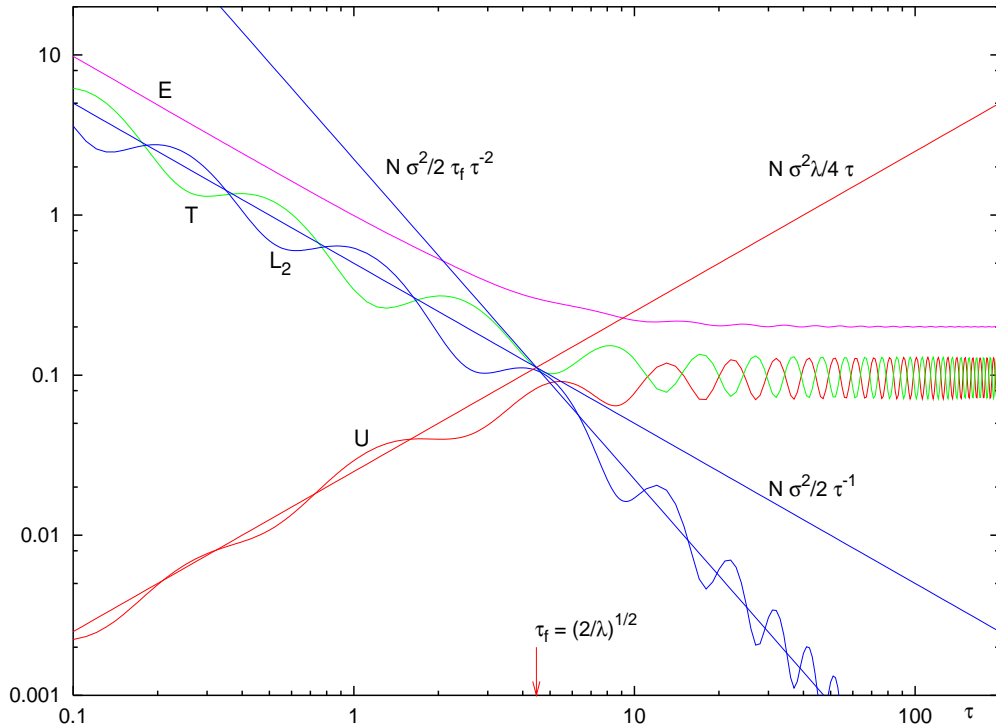


FIG. 1: Evolution on an $N = 100$ lattice of a single event according to EOM (6) in the Φ^4 -model with the $V^{(+)}$ symmetric potential ($\lambda = 0.1$). The initial distribution at $\tau = \tau_0$ is Gaussian (38) with $\sigma = 0.1$. The transition time τ_f is defined by the intersection of the lines $N\sigma^2/(2\tau)$ and $N\sigma^2\lambda\tau/4$.

For times $\tau \gg \tau_f$, the gradient terms become irrelevant. If, for large τ , we neglect in the EOM (6) the gradient terms altogether, then the fluctuations satisfy the simplified EOM

$$\frac{1}{\tau} \partial_\tau \phi + \partial_{\tau\tau} \phi + \lambda \phi = 0 \quad (46)$$

which is solved by

$$\phi \sim \frac{1}{\sqrt{\tau}} \cos(\sqrt{\lambda}\tau - \pi/4) + \mathcal{O}(\tau^{-1}), \quad (47)$$

i.e., the amplitudes of the fluctuations decrease like $1/\sqrt{\tau}$. This implies that both, $U^{(+)}$ and T , oscillate with constant amplitude, and frequency $2\sqrt{\lambda}$, both adding up to an asymptotically constant $E_\infty = T + U^{(+)}$, while L_2 rapidly decreases like $1/\tau^2$.

So, for times $\tau \gg \tau_f$, we are left with a system dominated by non-propagating fluctuations, or, in other words, with a system of N independently moving oscillators, all fluctuating with the same frequency $\sqrt{\lambda}$ (the 'mass' at $\Phi = 0$) and amplitudes decreasing like $1/\sqrt{\tau}$. Asymptotically for large proper times the total energy is conserved, realizing case (B2) discussed above.

Figure 1 shows the typical features of an evolution in the $V^{(+)}$ -potential (for $\lambda = 0.1$ and $\sigma = 0.1$). As long as $\tau_0 \ll \tau_f$, the actual choice of τ_0 and the initial values of $\partial_\tau \Phi_i(\tau = \tau_0)$ are unimportant. So, in contrast to our original expectations, the evolution shows very distinctly a transition from the early gradient-dominated phase to a system of N independent oscillators dominated by the local potential. In the first phase we observe the virial theorem $\langle T \rangle = \langle L_2 \rangle$, in the second phase we have $\langle T \rangle = \langle U \rangle$. At the transition time $\tau = \tau_f$, which is independent of σ and τ_0 , $\langle L_2 \rangle$ changes continuously from the τ^{-1} to $\tau_f \tau^{-2}$ behaviour.

The order of magnitude of τ_f can be obtained from the following argument: In the Bjorken frame, the field fluctuations carry an effective wave number k/τ and mass $\sqrt{\lambda}$. If k were not limited from above, then for any τ there could be propagating waves with $(k/\tau)^2 \geq \lambda$. However, if the system is characterized by a momentum cut-off, $k < \Lambda$, then for $\tau^2 \gg \Lambda^2/\lambda$, the system decouples into N independent oscillators with the same frequency $\sqrt{\lambda}$. On the lattice, k is limited by the finite lattice constant a : $k < \pi/a$. So, (with a put to 1), this provides an estimate for the freeze-out time τ_f . The statistical average over the initial ensemble then leads to (45). From this consideration we conclude that the observed freeze-out is the consequence of a momentum cut-off, which in the present case is imposed by the lattice. We should, however, keep in mind that here the lattice constant has a well-defined physical meaning: With our choice of the initial ensemble, where values of the field variables Φ_i at neighbouring lattice sites are uncorrelated, the lattice constant can be identified with the initial correlation length ξ . So, in this case, the freeze-out time should rather be written as

$$\tau_f^2 = \frac{2}{\lambda \xi^2}. \quad (48)$$

2. Potential with broken symmetry

Let us now consider an evolution subject to the potential V (31), which is characterized by two degenerate minima at $\Phi = \pm 1$ and satisfies $V(\pm 1) = 0$. As before, for sufficiently small width $\sigma \ll 1$ of the initial distribution, the potential is unimportant during the early phase of an evolution. So, starting from the same initial distribution as described above, the first part of an evolution proceeds exactly as in the case of the symmetric potential $V^{(+)}$ (37). The smooth part of the integral $U^{(-)} = \tau \int V^{(-)} d\eta = \tau \int (V(\Phi) - V(0)) d\eta$ again is approximated by

$$\langle U^{(-)} \rangle = (-)N \frac{\lambda}{4} \sigma^2 \tau, \quad (49)$$

while $\langle L_2 \rangle$ is still given by (44). So, the freeze-out time τ_f as determined from

$$-\langle U^{(-)} \rangle = \langle L_2 \rangle \quad (50)$$

again is given by (45). (Due to the opposite sign of $\langle U^{(-)} \rangle$ as compared to the case of the symmetrical potential $\langle U^{(+)} \rangle$, this condition here implies that even for the highest wave numbers $k \sim 1/a$ supported by the lattice, the frequencies become imaginary for $\tau > \tau_f$).

For $\tau > \tau_f$, the gradients which couple the field variables Φ_i at neighbouring lattice sites are suppressed and the onset of the potential drives each Φ_i towards $+1$ or -1 , depending only on the sign of Φ_i at $\tau \sim \tau_f$. So, evidently, τ_f is also that point in time when the number n of kinks+antikinks finally found in the system for $\tau \rightarrow \infty$ is determined. Necessarily, because for $\tau > \tau_f$ the Φ_i at neighbouring sites no longer interact, the analytical shape of the stable (shrinking) kink is irrelevant, or, in other words, the size $R = \left(\tau \sqrt{\lambda/2}\right)^{-1}$ of the kinks has shrunk below the lattice unit. This provides another interpretation of the freeze-out time which we could have chosen alternatively to define

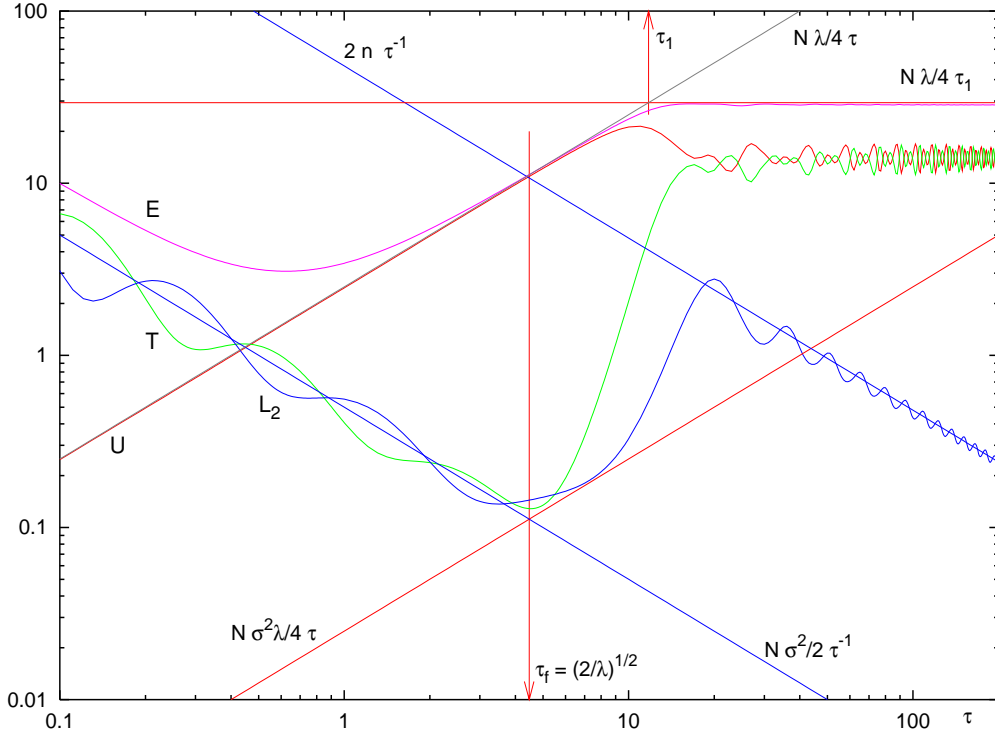


FIG. 2: Evolution on an $N = 100$ lattice of a single event (with $\sigma = 0.1$) according to EOM (6) in the Φ^4 -model with the broken-symmetry potential $V(\Phi)$ (31) (for $\lambda = 0.1$). The freeze-out time $\tau_f = \sqrt{2/\lambda} = 4.47$ is defined as in figure 1 by the intersection of the lines $N\sigma^2/(2\tau)$ and $N\sigma^2\lambda\tau/4$. The number n of kinks+antikinks remaining in the final configuration is tied to the intersection of the lines $2n/\tau$ and $N\lambda\tau/4$. This particular event leads to $n = 24$. The arrow at $\tau = \tau_1$ points to the end-of-roll-down time as given by eq. (71). Its intersection with the line $N\lambda\tau/4$ marks the finally available energy E_∞ (in the approximation discussed in subsection III.E).

τ_f . Clearly, for $R < 1$, kinks and antikinks no longer overlap, so there is no further annihilation and their total number n is conserved.

Figure 2 shows the typical features of an evolution in the symmetry-broken potential V (31) (for $\lambda = 0.1$), starting from an initial Gaussian distribution with $\sigma = 0.1$. For proper times larger than the freeze-out time, $\tau > \tau_f = \sqrt{2/\lambda}$, L_2 switches from oscillating around $N\sigma^2/(2\tau)$ to oscillating around $2n/\tau$ (with $n = 24$ in this particular example), while U begins to deviate from $N\lambda\tau/4$ and joins with T into combined oscillations around the constant $E_\infty/2$. These fluctuations consist of the N Φ_i -values oscillating independently around the vacua $\Phi = \pm 1$ with frequency $\omega_0 = \sqrt{2\lambda}$ (the 'mass' in the true vacuum) and amplitudes decreasing like $1/\sqrt{\tau}$, so U and T asymptotically oscillate with frequency $2\omega_0$ with constant amplitudes.

We can obtain an estimate for the number n by the following consideration: As given in (36), for large proper times $\tau \gg \tau_f$ we expect L_2 to approach the limit $\langle L_2 \rangle = 2n/\tau$ which on the lattice comprises the kinks' contribution to the energy. For proper times up to τ_f , $\tau < \tau_f$, the integral $\int V d\eta$ is dominated by the constant contribution $V(0)$, i.e. we have $\langle U \rangle = N\lambda\tau/4$. Both constants, $V(0)$ before the transition, and $2n$ after the transition, do not enter into the EOM which describes the fluctuations around them and which determines the transition time τ_f . In normal time t , energy conservation would require both constants to be equal. To translate that into the proper-time frame, we have to extrapolate $\langle L_2 \rangle$ backwards to the freeze-out time τ_f and consider its intersection with $\langle U \rangle$ at τ_f

$$\langle U \rangle = \langle L_2 \rangle |_{\tau=\tau_f} \quad \text{i.e.} \quad N\frac{\lambda}{4}\tau_f = 2n\frac{1}{\tau_f}. \quad (51)$$

So we obtain as an estimate for the number n of kinks+antikinks expected to survive,

$$n = \frac{N}{4}. \quad (52)$$

For this consideration the fluctuational contributions to U and to L_2 are unimportant because they are suppressed by order $\mathcal{O}(\sigma^2)$, (apart from the fact that they determine τ_f). The result (52) is very simple and independent of λ (and

of σ and τ_0 , if chosen sufficiently small). It may be noted that it is just one half of the purely statistical Kibble limit $n_K = N/2$. Numerically, it can be measured as the average kink+antikink number \bar{n} obtained for a large ensemble of events. Averaging over 1000 events we find a slight dependence on τ_0 and σ : for $N = 100$, $\sigma = 0.01$ and $\tau_0 = 0.1, 0.01$ we have $\bar{n} = 25.0(4.7), 27.6(5.0)$; for $\sigma = 0.1$ and $\tau_0 = 0.1, 0.01$ we find $\bar{n} = 26.1(4.7), 28.9(5.1)$, respectively. (Cf. figs.6 and 7). (The numbers in brackets give the corresponding mean deviations).

Although the momentum cut-off implemented through the lattice (which is decisive for the freeze-out time and instrumental for the occurrence of the transition) can have a genuine physical meaning, it is still unsatisfactory that the shrinking kinks' contribution to the energy, due to the finite lattice constant, is given by $2n/\tau$, and not by their true energy (35) $E = n \cdot 2\frac{\sqrt{2\lambda}}{3}$ which is independent of τ . To correct for that lattice artifact we can replace (51) by

$$N\frac{\lambda}{4}\tau_f = 2n\frac{\sqrt{2\lambda}}{3} \quad (53)$$

and, with (45), obtain the result

$$n = \frac{3}{8}N \quad (54)$$

which again is independent of λ . We shall see in the following that this is the appropriate procedure, if the freeze-out occurs before the soliton size has shrunk to the lattice-unit.

C. Temperature and initial distributions

We have seen from the preceding results that the momentum cut-off $\Lambda = \pi/a$, here imposed on the system by the finite lattice constant a , is crucial for the freeze-out time and for the onset of the phase transition. Although, for the initial configurations chosen, the lattice constant does acquire physical meaning as the initial correlation length, it may seem very unsatisfactory that the essential physical processes rely on a rather arbitrarily chosen momentum cut-off. Therefore it is more natural to introduce a cut-off $\Lambda\mathcal{T}$ through a temperature \mathcal{T} characterizing the initial distribution. For this purpose we construct the initial configurations Φ_i ($i = 1, \dots, N$) on the lattice, as Fourier transforms

$$\Phi_i = \sqrt{2/N} \sum_{k=1}^N \sin\left(\frac{\pi}{N}k \cdot i\right) \tilde{\Phi}_k$$

of distributions $\tilde{\Phi}_k$ ($k=1, \dots, N$) in momentum space, chosen randomly from a Gaussian deviate $f_G(\tilde{\Phi})$ with k -dependent width σ_k ,

$$f_G(\tilde{\Phi}_k) = \frac{1}{\sqrt{2\pi\sigma_k^2}} \exp\left(-\frac{\tilde{\Phi}_k^2}{2\sigma_k^2}\right), \quad \text{with} \quad \sigma_k^2 = \frac{\sigma_0^2}{\sqrt{2\pi\sqrt{\lambda}\mathcal{T}}} \exp\left(-\frac{(k\pi/(aN))^2}{2\sqrt{\lambda}\mathcal{T}}\right). \quad (55)$$

In other words, we choose a Boltzmann distribution for the average occupation numbers $\langle n_k \rangle = \langle \tilde{\Phi}_k^2 \rangle = \sigma_k^2$ for particles with mass $\sqrt{\lambda}$ (i.e., the 'mass' of the fluctuations in the symmetric potential $V^{(+)}$) and temperature \mathcal{T} . On a lattice, the upper limit for k is N . So, as long as

$$\mathcal{T} < \Lambda\mathcal{T}, \quad \text{with} \quad \Lambda\mathcal{T} = \frac{\pi^2/a^2}{2\sqrt{\lambda}}, \quad (56)$$

the lattice cut-off is unimportant. With $a = 1, \lambda = 0.1$ we have $\mathcal{T} < 15.6$. Within that limit we obtain for the width of the initial distribution of the field configurations Φ_i on the 'coordinate' lattice

$$\sigma^2 = \langle \Phi^2 \rangle = \frac{1}{N} \sum_k \langle \tilde{\Phi}_k^2 \rangle = \frac{\sigma_0^2}{2\pi}, \quad (57)$$

which even for $\sigma_0^2 = 1$ still is smaller than 1. So, our previous arguments which lead to $|\langle U^{(\pm)} \rangle| = N\sigma^2\lambda/4\tau$ still hold and we obtain in place of (49)

$$|\langle U^{(\pm)} \rangle| = N\lambda \frac{\sigma_0^2}{8\pi}\tau. \quad (58)$$

For an estimate of $\langle L_2 \rangle$, as in equation (42) we need the correlation function $\langle \Phi_{i+1} \Phi_i \rangle$, which now no longer factorizes, but instead is given by

$$\frac{1}{N} \sum_{i=1}^N \langle \Phi_{i+1} \Phi_i \rangle = \frac{\sigma_0^2}{2\pi} \exp\left(-\sqrt{\lambda}\mathcal{T}/2\right). \quad (59)$$

So, together with (57) we obtain for $\langle L_2 \rangle$

$$\langle L_2 \rangle = \frac{N\sigma_0^2}{4\pi\tau} \left(1 - \exp\left(-\sqrt{\lambda}\mathcal{T}/2\right)\right). \quad (60)$$

We again use $|\langle U^{(\pm)} \rangle| = \langle L_2 \rangle$ to get the freeze-out time

$$\tau_f^2 = \frac{2}{\lambda} \left(1 - \exp\left(-\sqrt{\lambda}\mathcal{T}/2\right)\right). \quad (61)$$

If we use as an estimate for the average kink+antikink multiplicities n the relation (51) we find

$$n = \frac{N}{4} \left(1 - \exp\left(-\sqrt{\lambda}\mathcal{T}/2\right)\right). \quad (62)$$

However, for small temperatures \mathcal{T} , the freeze-out time (61) will be much shorter than the time $\sqrt{2/\lambda}$ when the kinks' size approaches the lattice unit. So it appears more appropriate to replace (51) by (53), which accounts for the fact that at times $\tau < \sqrt{2/\lambda}$ the emerging (and shrinking) kinks' energy is constant and given by $2\frac{\sqrt{2\lambda}}{3}$. This leads to

$$n = N\frac{3}{8} \left(1 - \exp\left(-\sqrt{\lambda}\mathcal{T}/2\right)\right)^{1/2}. \quad (63)$$

For small temperatures this results in a square-root law for the multiplicities $n/N = \frac{3}{8\sqrt{2}}\sqrt{\sqrt{\lambda}\mathcal{T}}$.

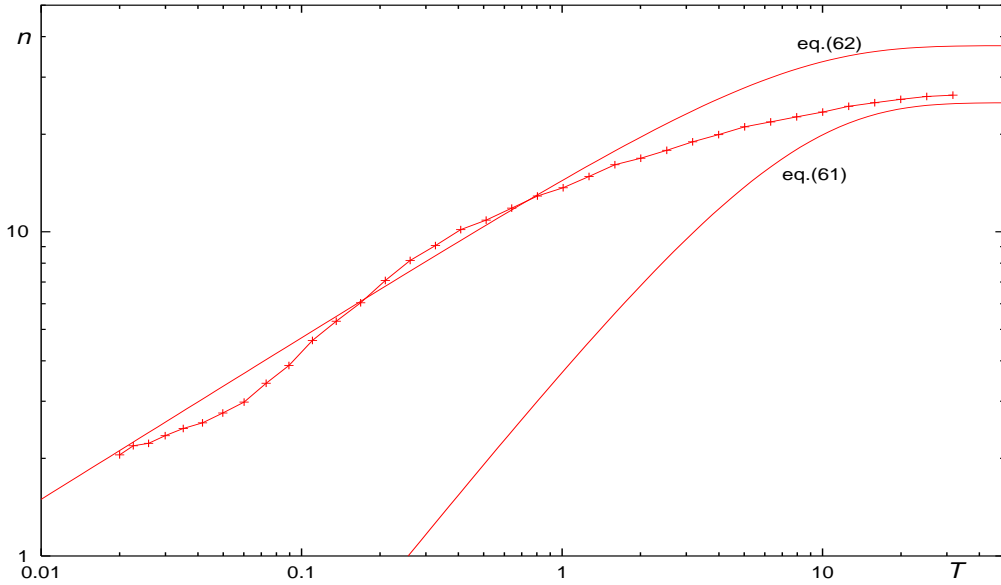


FIG. 3: Kink+antikink multiplicities \bar{n} (averaged over 500 events) as function of the initial temperature \mathcal{T} (for $N = 100, \lambda = 0.1$). The solid lines are calculated from the expressions (62) and (63), respectively.

In figure 3 we compare the numerically measured \bar{n} (averaged over 500 events, $N = 100, \lambda = 0.1$) as function of initial temperature \mathcal{T} with both expressions, (62) and (63). Evidently, using the shrinking kink's true constant energy $2\frac{\sqrt{2\lambda}}{3}$, provides a good approximation for \bar{n} in the low-temperature region, while the use of the lattice expression $2/\tau$ describes only the limit where the temperature exceeds the cut-off $\Lambda\tau$ in (56). These results show that our expressions for the freeze-out time and the multiplicities n work reasonably well, independently of the physical origin of the momentum cut-off. We shall therefore in the following return to the simple case where the momentum-cut-off is provided by the lattice constant.

D. Cooling times

Up to now we have considered the 'sudden quench', i.e. the initial 'hot' configuration was exposed from the outset $\tau \geq \tau_0$ to a fixed potential. In general, however, the Φ^4 -potential would be of a form like

$$V(\Phi) = \frac{\lambda}{4}(\Phi^2 - v^2(\tau))^2 \quad (64)$$

with a time- (or temperature-) dependent function $v^2(\tau)$ to drive the phase transition. Typically, the functional dependence of v^2 on proper time τ would be like

$$v^2(\tau) = \tanh(\tau/\tau_c - 1), \quad (65)$$

parametrized by a cooling time τ_c which characterizes the time it takes the potential to approach its 'cold' form. A possible scenario how the time-scale of this change in the effective chiral potential may be driven by a confining transition coupled to it has been discussed in the rapidly expanding Bjorken metric in [21]. In the present context, however, we shall simply impose a suitable time dependence like (65).

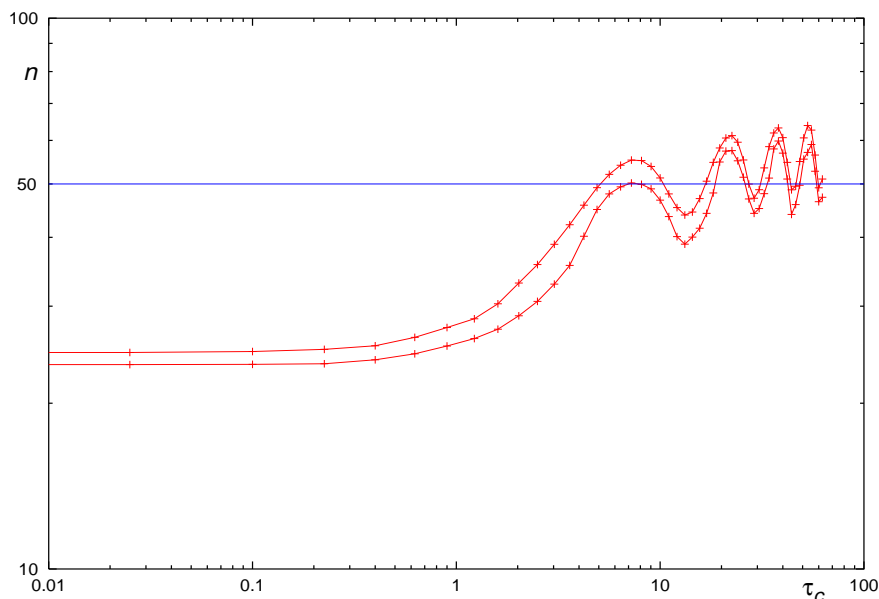


FIG. 4: Kink+antikink multiplicities \bar{n} (averaged over 500 events) as function of cooling time τ_c (for $N = 100, \lambda = 0.1$, and for two different choices of the initial width $\sigma = 0.0001$ and $\sigma = 0.01$). The frequency of the oscillations around $n = N/2$ is $\omega = \sqrt{2\lambda}$.

We have seen that in the Bjorken frame for a fixed potential the kinetic freeze-out time $\tau_f = \sqrt{2/\lambda}$ in (45) is obtained independently of the sign of v^2 , being solely determined by the coupling constant λ and the momentum cut-off which characterizes the system. Retracing our arguments which have lead to equations (41) and (49), now for the τ -dependent potential (64), we obtain for the freeze-out time

$$\tau_f^2 = \frac{2}{\lambda v^2(\tau_f)} \quad (66)$$

For an ansatz like (65) the solutions τ_f^2 of this equation satisfy $\tau_f^2 > 2/\lambda$. They approach the lower limit $2/\lambda$ for $\tau_c \rightarrow 0$. For very long cooling times $\tau_c \rightarrow \infty$, we have $\tau_f/\tau_c \rightarrow 1$. In any case, if τ_c is smaller or comparable to $\sqrt{2/\lambda}$, then also the freeze-out time τ_f is comparable to $\sqrt{2/\lambda}$ and we can apply equation (51) which determines the kink multiplicities. With the potential (64) this is now modified as

$$N \frac{\lambda}{4} v^4 \tau_f = \frac{n}{2} (2v^2)^2 \frac{1}{\tau_f}. \quad (67)$$

So, with (66), we obtain the same result $n = N/4$ as before, independently of the value of $v^2(\tau_f)$. We conclude, that as long as the cooling time τ_c is smaller than the kinetic freeze-out limit $\sqrt{2/\lambda}$, the resulting multiplicities are almost independent of τ_c , and it is justified to use the sudden quench approximation $\tau_c = 0$.

This is no longer true for $\tau_c \gg \sqrt{2/\lambda}$. In that case the potential (64) is still symmetric with a single ($\Phi = 0$) minimum at the time $\tau = \sqrt{2/\lambda}$ when all modes decouple. Therefore, by the time $\tau = \tau_c$ when the potential develops its degenerate true minima with broken symmetry, all field variables Φ_i roll down into the nearest minimum, independently of each other. So, for large cooling times, the average number \bar{n} will approach the Kibble limit $N/2$. Figure 4 shows kink+antikink multiplicities \bar{n} (averaged over 500 events) as function of cooling time τ_c (for $\lambda = 0.1$, and for two different choices of the initial width $\sigma = 0.0001$ and $\sigma = 0.01$). The fact that \bar{n} oscillates with $\omega = \sqrt{2\lambda}$ (the 'cold' mass) shows that the roll down proceeds only after the potential has essentially reached its final 'cold' form.

Physically, this is not interesting because the field variables Φ_i at different lattice sites do not interact with each other for $\tau \gg \sqrt{2/\lambda}$. We therefore in the following consider only the sudden quench $\tau_c = 0$.

E. Evolution after freeze-out

At freeze-out the energy present in the rapidity interval is completely converted into kink-antikink pairs. After freeze-out the roll-down sets in, i.e. the field evolution is dominated by the potential. Locally, the field picks up kinetic energy T under the influence of the potential $-\frac{\lambda}{2}\Phi^2$ (for $|\Phi| \ll 1$). As long as $|\Phi|$ is sufficiently small the equation of motion is

$$\frac{1}{\tau}\dot{\Phi} + \ddot{\Phi} - \lambda\Phi = 0, \quad (68)$$

solved by

$$\Phi(\tau) = c I_0(\sqrt{\lambda}\tau) = c \exp(\sqrt{\lambda}\tau)F(\sqrt{\lambda}\tau). \quad (69)$$

with $F(x)$ a slowly monotonically decreasing function of x . If σ is the (average) length of Φ at τ_f , then the constant c is $c = \sigma/I_0(\sqrt{\lambda}\tau_f)$. For the typical roll-down time τ_1 we take the time when $|\Phi(\tau_1)| = 1$ is reached. So, we have

$$\sqrt{\lambda}(\tau_1 - \tau_f) = -\ln \sigma + \ln \frac{F(\sqrt{\lambda}\tau_f)}{F(\sqrt{\lambda}\tau_1)}. \quad (70)$$

As a first approximation we use

$$\tau_1 - \tau_f = -\frac{1}{\sqrt{\lambda}} \ln \sigma. \quad (71)$$

(This is a lower limit, because the omitted last term in (70) is > 0 , and because for $|\Phi| \sim 1$ the 4-th order terms in V become important. But for an estimate, (71) is good enough. The estimate should be best for small σ .) During this time interval the spatial volume covered by the Bjorken slab grows linearly with proper time.

The local energy density is dominated by the constant $\lambda/4$, so by the end of the roll-down the additional energy $(\tau_1 - \tau_f)N\lambda/4$ is available to be converted into σ -fluctuations around the true vacua $\Phi = \pm 1$. These fluctuations carry the mass $\omega_0 = \sqrt{2\lambda}$. So, at the end of the evolution, in addition to the n (anti)kinks formed at freeze-out time, we find σ -mesons emitted from the considered rapidity slab with multiplicity

$$n_\sigma = \frac{N\lambda}{4} \frac{(-1)}{\sqrt{\lambda}} \ln \sigma \frac{1}{\sqrt{2\lambda}} = -\frac{N \ln \sigma}{4\sqrt{2}}. \quad (72)$$

Altogether, with $n = N/4$ from (52) we obtain for the multiplicity ratio of baryon-antibaryon pairs to σ -mesons

$$\frac{n/2}{n_\sigma} = -\frac{1}{\sqrt{2} \ln \sigma} \quad (73)$$

which is independent of the coupling constant λ .

In fig.(2), in addition to the arrow at freeze-out time $\tau_f = \sqrt{2/\lambda} = 4.47$ another arrow shows the end-of-roll-down time $\tau_1 = \tau_f + \sqrt{10} \ln 10 = 11.75$, as given in (71) for $\lambda = 0.1, \sigma = 0.1$. Its intersection with the linearly rising

$U(\Phi = 0)$ defines the energy $N\lambda\tau_1/4$ available at $\tau = \tau_1$. It can be seen in fig.(2) that the straight horizontal line through this intersection coincides very closely with the actual numerically calculated total energy E for times $\tau > \tau_1$. (The contribution $2n\tau^{-1}$ of the kinks is negligible (on the lattice) for $\tau > \tau_1$).

The last equation (73) holds for the initial configurations as described in (38). If we use the initial conditions (55) which involve a temperature cut-off in momentum space, we have instead, with (63), (72) and (57)

$$\frac{n/2}{n_\sigma} = -\frac{3\sqrt{2}}{4\ln\sigma}(1 - \exp(-\sqrt{\lambda\mathcal{T}}/2))^{1/2}. \quad (74)$$

For small values of $\sqrt{\lambda\mathcal{T}}$ this reduces to

$$\frac{n/2}{n_\sigma} = -\frac{3}{4\ln\sigma}(\sqrt{\lambda\mathcal{T}})^{1/2}. \quad (75)$$

With the potential of the true vacuum at $\Phi = \pm 1$ put to zero, after the roll-down there is no further linear rise in the total energy of the expanding Bjorken slab. Remarkably, the $\tau^{-1/2}$ law (47) of the amplitudes of the remaining vacuum fluctuations provides an asymptotically constant total energy $E(\tau \rightarrow \infty) = E_\infty$, similar to the asymptotically constant (exact) energy stored in the shrinking kinks.

F. Including an explicitly dissipative term

We have seen that in the Bjorken frame the onset of a phase transition, together with the freeze-out of independent kinks, antikinks, and 'mesonic' fluctuations around the true vacua, is basically governed by the momentum cut-off which characterizes the system. The 'cooling' of the system originates in the decrease of effective wave numbers k/τ with increasing proper time τ . In addition to this kinetic cooling we normally would expect also genuine physical cooling to occur due to radiative processes which dissipate energy from the excited system into the surrounding vacuum.

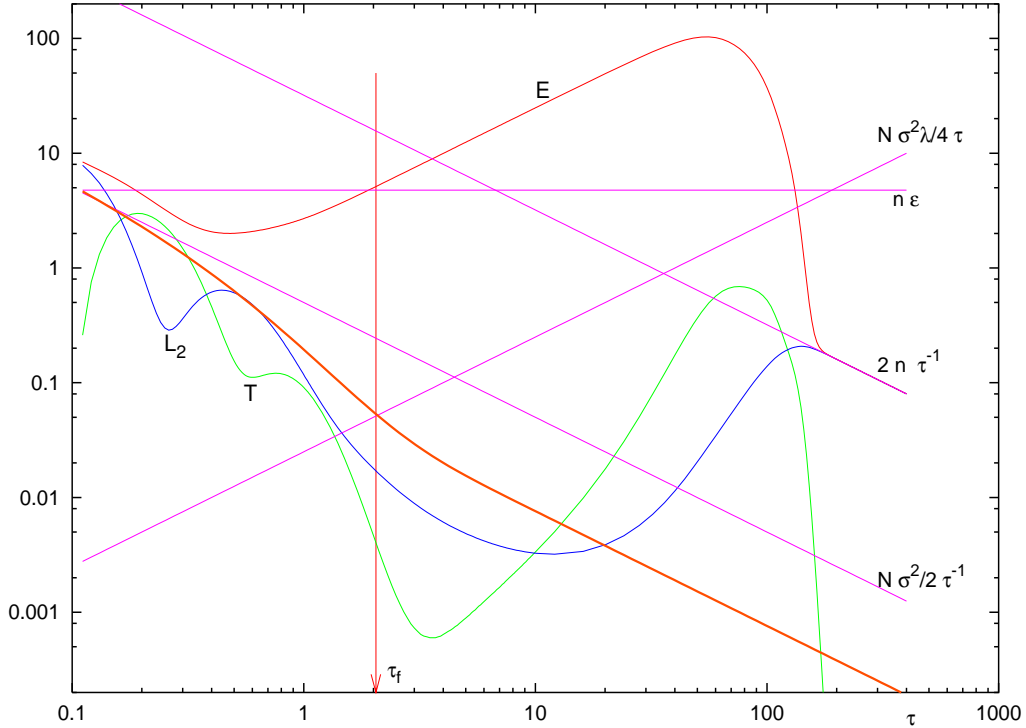


FIG. 5: Evolution ($N = 100, \lambda = 0.1, \tau_0 = 0.1, \sigma = 0.1$) according to EOM (19) with additional dissipation ($\gamma = 2$). The thick solid line shows the expression (27)(for $\alpha = 1/2$) for the smooth part $\langle L_2 \rangle$. It intersects $|\langle U^{(-)} \rangle| = (N/4)\lambda\sigma^2\tau$ at freeze-out time $\tau_f = 2.05$. This event produces $n = 16$ kinks+antikinks. The constant 16ϵ with $\epsilon = 2\frac{\sqrt{2\lambda}}{3}$ intersects the total energy E near freeze-out time τ_f . The line $16 \cdot 2/\tau$ dominates the energy for $\tau > 200$.

We incorporate this effect by including a finite dissipation constant γ into the EOM (19) as described in section II.C. During the early phase of an evolution, up to the onset of a transition, this does not affect the linear rise of $\langle U \rangle$. On the other hand, the dissipation damps away the rapidity and proper time gradients such that their smooth sum $T + L_2$ drops below the $N\sigma^2/\tau$ line. Therefore the freeze-out time τ_f is reduced as compared to the case $\gamma = 0$. Correspondingly, the average number \bar{n} of kinks+antikinks produced is also reduced. As an example, figure 5 shows the evolution of one event for $\gamma = 2$ (with $\sigma = 0.1, \tau_0 = 0.1$). This event leads to $n = 16$ kinks+antikinks. Applying the approximation (27) (with $\alpha = 1/2$) for an average $\langle L_2 \rangle$, (which in figure 5 is shown by the solid line), we find as in (50) from its intersection with the linearly rising $|\langle U^{(-)} \rangle| = (N/4)\lambda\sigma^2\tau$ the freeze-out time $\tau_f = 2.05$ (as compared to $\tau_f = \sqrt{2/\lambda} = 4.47$ for $\gamma = 0$). At this early time the emerging kinks have not yet shrunk to lattice-unit size, so we use their true constant energy $\varepsilon = 2\sqrt{2\lambda}/3$ to extract from the total energy E at time τ_f their multiplicity $n = E(\tau_f)/\varepsilon$. In figure 5 this is indicated by the horizontal line at 16ε , which may be seen to intersect E (which near τ_f is dominated by the linear rise of potential $\langle U \rangle$) near proper time τ_f . The roll-down phase which follows for $\tau > \tau_f$ is characterized by a peak in the proper time derivatives T , followed by a rapid decrease in U , as the configuration settles in the true vacua. Finally the total energy is dominated by the (lattice-artifact kink energies) $n \cdot 2/\tau$ behaviour of L_2 for $n = 16$. During and after the roll-down phase all fluctuations have been damped away by the dissipative term.

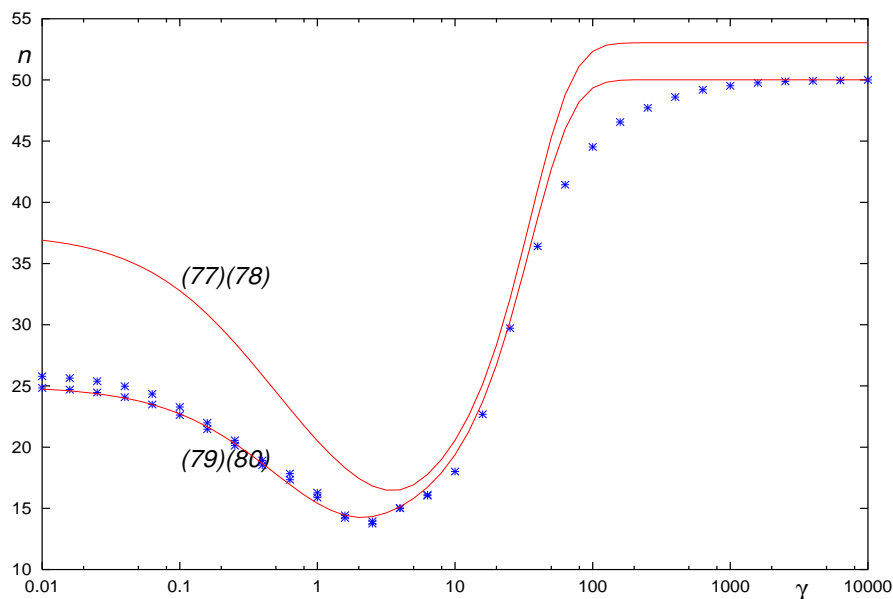


FIG. 6: Numerically measured kink+antikink multiplicity \bar{n} (averaged over 1000 random events) as functions of damping constant γ for initial time $\tau_0 = 0.1$ (and two values for the width of the initial distribution $\sigma = 0.1$ and $\sigma = 0.01$). The solid lines show the results (for $\alpha = 1/2$) of the analytical approximations eqs. (77),(78) and (79),(80), respectively.

This pattern changes for very large values of the dissipation constant γ . As $\gamma\tau_0$ approaches unity, the proper time derivatives T get strongly suppressed already from the beginning of the evolution such that T stays small and L_2 dominates the total energy. For $\gamma\tau_0 \gg 1$, L_2 is determined by its initial value alone, it approaches the line

$$L_2 = N \frac{\sigma^2}{\tau}, \quad (76)$$

i.e. it takes twice the value (44) it has for $\gamma = 0$. Correspondingly, the average number \bar{n} of kinks+antikinks approaches the Kibble limit $\bar{n} \rightarrow N/2$. In other words, the field configuration is basically frozen from the very beginning at $\tau = \tau_0$, the evolution consists only of the field variables Φ_i at each lattice point drifting to the nearest true minimum at $\Phi = \pm 1$. So, in that limit, the notion of a freeze-out time becomes meaningless.

Still it is interesting to employ the analytical expression (27) for $\langle L_2 \rangle$ to determine τ_f from

$$\frac{N\sigma^2}{\tau_f} \frac{(1 + e^{-\alpha\gamma\tau_f})^{2/\alpha-1}}{(1 + e^{-\alpha\gamma\tau_0})^{2/\alpha}} = N\sigma^2 \frac{\lambda}{4} \tau_f, \quad (77)$$

and the number n of kinks+antikinks from (53)

$$n = \frac{3}{8} N \sqrt{\frac{\lambda}{2}} \tau_f. \quad (78)$$

This provides the limits $n \rightarrow 3N/8$ for $\gamma \rightarrow 0$, and $n \rightarrow 3N\sqrt{2}/8$ for $\gamma\tau_0 \gg 1$ and a minimum of n near $\gamma\tau_0 \sim 0.5$. Figure 6 shows the resulting n as function of the dissipation constant γ , for $\alpha = 1/2$, in comparison with the numerically measured \bar{n} (averaged over 1000 events, for $\lambda = 0.1$, $\tau_0 = 0.1$ and two values for the width of the initial distribution $\sigma = 0.1$ and $\sigma = 0.01$). Although the general features of \bar{n} are nicely reproduced, the limits for $\gamma \rightarrow 0$ and $\gamma\tau_0 \gg 1$ are not correct. This is no surprise because in both limits the true kink energy ε should be replaced by the lattice result, i.e. (78) should be replaced by (51)

$$n = N \frac{\lambda}{8} \tau_f^2. \quad (79)$$

This then leads to the correct (lattice) limits $n \rightarrow N/4$ for $\gamma \rightarrow 0$, and $n \rightarrow N/2$ for $\gamma\tau_0 \gg 1$. It is interesting to note that a quite satisfactory parametrization of the results can be obtained by using (79) for all values of γ , but replacing $< L_2 >$ on the left-hand side of (77) by

$$\frac{1 + e^{-\alpha\gamma\tau_f}}{\tau_f (1 + e^{-\alpha\gamma\tau_0})^2} = \frac{\lambda}{4} \tau_f. \quad (80)$$

This comparison is also shown in fig.6, again for $\alpha = 1/2$. Evidently, it provides remarkably good agreement for γ -values up to $\gamma\tau_0 < 5$.

G. Adiabatic approximation

For large values of the dissipation constant γ it should be sufficient to employ the adiabatic approximation as described in section II.D. Evolving the initial configurations with the purely dissipative EOM (28), leads to the kink+antikink multiplicities \bar{n} (averaged over 1000 events, for $N = 100$, and $\lambda = 0.1$) shown in figure 7 for two initial times $\tau_0 = 0.1, 0.01$ (and initial Gaussian width $\sigma = 0.01$). For comparison, the non-adiabatic results for the same two cases are included.

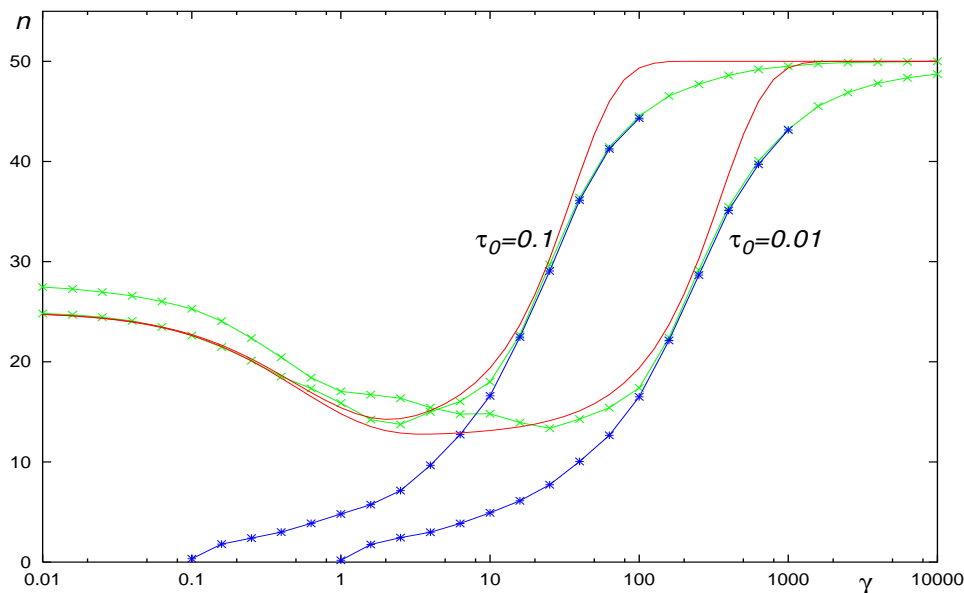


FIG. 7: Numerically measured kink+antikink multiplicities \bar{n} (averaged over 1000 random events) as functions of damping constant γ for two different initial times $\tau_0 = 0.1, 0.01$ (and initial width $\sigma = 0.01$) as obtained from the adiabatic EOM (28). For comparison, the non-adiabatic results are also included. The solid lines show the result of the analytical approximation (79),(80) (with $\alpha = 1/2$) for the same two cases.

It is apparent that the adiabatic approximation works very well for $\gamma\tau_0 > 1$. It can also be observed that for $\gamma\tau_0 < 10^{-2}$ the adiabatic evolutions produce no kinks at all, i.e. the configurations become so smooth at a very early time (when the 'size' of the kinks is still very large), such that the complete configuration rolls down into the same true minimum. The solid lines show the result of the analytical approximation (79),(80) for both cases $\tau_0 = 0.1, 0.01$.

IV. CONCLUSION

The dynamics of interacting fields in rapidly expanding systems is characterized by effective wave numbers decreasing with time. This is conveniently modeled by transforming from space-time (x, t) to the rapidity - proper-time (η, τ) (Bjorken) frame. In the equations of motion for the evolving fields, the rapidity gradients then explicitly carry the inverse proper-time factors, and an additional first-order proper-time derivative term appears which resembles dissipative dynamics, although no genuine physical dissipation is present. In the (η, τ) frame, the system still is characterized by a lagrangian which, however, explicitly depends on proper time. So, the energy is not conserved, but may decrease or rise during the evolution of a field configuration. This is especially interesting for those cases where the system is able to undergo a 'phase transition', where initial configurations through a cooling process settle down into the true vacua. Usually, cooling or heating is provided by energy exchange with external degrees of freedom (heat bath), but in the (η, τ) frame the transition is solely driven by proper time.

Systems characterized by multiple different degenerate vacua are of specific interest because during the course of the phase transition it must be decided how the different vacua get populated. Field configurations connecting different vacua will finally show up as defects, kinks, or solitons, and their multiplicities can be physically significant and observable.

The mechanism of how the transition is effectuated by proper time in the Bjorken frame is quite transparent. The term which comprises the (rapidity-)gradients contribution L_2 to the total energy carries a factor $1/\tau$, while the potential-energy part U carries a factor τ . Therefore, the evolutions at very early times will be dominated by L_2 independently of the potential, while, if the gradients in the field configurations are limited by a momentum-cut-off Λ , then for very late times the gradients will become unimportant, propagation in rapidity space will end, and the field variables evolve locally according to the local potential. Evidently, there will exist a freeze-out time τ_f which separates both regimes. It is conveniently defined as the time when L_2 equals U (where suitable care has to be taken to subtract eventual constants in the definition of the interaction). Clearly, the momentum cut-off (or the finiteness of L_2) is a necessary condition for the transition to occur, and the actual value of the freeze-out time will depend decisively on Λ . Therefore it is important that the momentum cut-off reflects a genuine physical characteristic of the initial field ensemble, typically an initial temperature or inverse correlation length. This then, however, implies that the freeze-out time can be calculated very simply from the initial ensemble.

Stable solitons in the Bjorken frame shrink with increasing proper time, or, in other words, their stable size relative to the expanding system decreases. But remarkably, their total energy is constant and equal to their static total energy in the usual (z, t) frame. This allows to estimate their multiplicities from the total energy available at freeze-out time (including eventual constants in the definition of the interaction). This means that we may obtain estimates for the average soliton(+antisoliton) multiplicities directly from the form of the initial ensemble and the static lagrangian which determines their mass.

A convenient way to introduce a momentum cut-off is to implement the system on a lattice. Then, however, we have to make sure that the lattice cut-off does not interfere with the increasing gradients which characterize the shrinking solitons at τ_f . Alternatively, we have to use the lattice expression for the soliton's energy if it has shrunk to lattice-unit size.

We have investigated these features in the (1+1)-dimensional Φ^4 -model. We find that the simple analytical expressions for τ_f and n agree very nicely with numerically measured freeze-out times and kink+antikink multiplicities. We have also used Boltzmann ensembles with temperatures well below and up to the lattice cut-off. Employing the appropriate correlation function we again find good agreement with the numerical averages. For low temperatures we obtain a square-root law $n \propto \sqrt{\mathcal{T}}$. For temperatures approaching the lattice cut-off the influence of the appropriate soliton energy becomes evident. We show that within the physically interesting region it is sufficient to consider the sudden quench where the initial ensemble is exposed from the beginning to the fixed cold potential. After the freeze-out the additional energy picked up by the expanding rapidity slice is converted into mesonic fluctuations. A simple estimate of the roll-down time provides an expression for their average multiplicities.

In addition to the 'free' evolutions in the Bjorken frame we have also investigated the inclusion of additional genuine dissipation with variable damping constant γ . It is very satisfactory to find that all the previous considerations can be applied to this case, that the decrease in the freeze-out times caused by the damping can be represented in simple analytical expressions and that the multiplicities n again reflect the soliton energies at freeze-out time. Finally we find that the validity of the adiabatic approximation, (where all second order time-derivatives are dropped), is limited

by $\gamma\tau_0 > 1$ where τ_0 denotes the proper time at which the initial ensemble is prepared and the evolution starts.

It will be most interesting to look at the corresponding features in the (3+1)-dimensional O(4)-model considered previously as a model for baryon-antibaryon production in relativistic heavy-ion collisions and compare the results with recent experimentally observed nucleon-antinucleon multiplicities and with statistical models. The scheme may also be useful for applications in cosmology.

Acknowledgments

The author appreciates many helpful discussions with Jorgen Randrup and Hendrik Geyer. He is especially indebted to Hans Walliser for a careful reading of the manuscript. It is a pleasure to thank the Nuclear Theory Group at Lawrence Berkeley Laboratory, and the Physics Department at Stellenbosch University for the warm hospitality extended to him.

-
- [1] J.D. Bjorken, Phys.Rev. **D27**, 140 (1983).
 - [2] STAR Collaboration, C. Adler *et al.*, Phys. Rev. Lett. **86**, 4778 (2001); **87**, 262302 (2001).
 - [3] BRAHMS Collaboration, I.G. Bearden *et al.*, Phys. Rev. Lett. **87**, 112305 (2001).
 - [4] BRAHMS Collaboration, I.G. Bearden *et al.*, Nucl. Phys. **698**, 667 (2002); nucl-ex/0207006.
 - [5] T.A. DeGrand, Phys. Rev. **D30**, 2001 (1984).
 - [6] J. Ellis and H. Kowalski, Phys. Lett. **B214**, 161 (1988).
 - [7] J. Ellis, M. Karliner, and H. Kowalski, Phys. Lett. **B235**, 341 (1990).
 - [8] J.I. Kapusta and S.M.H. Wong, Phys. Rev. Lett. **86**, 4251 (2001); J. Phys. **G28**, 1929 (2002).
 - [9] T.W.B. Kibble, J. Phys **A9**, 1387 (1976).
 - [10] N.H. Christ, R. Friedberg, and T.D.Lee, Nucl. Phys. **B202**, 89 (1982).
 - [11] G. Holzwarth, Phys. Rev. **D65**, 054013 (2002); **D59**, 105022 (1999).
 - [12] G. Holzwarth and J. Klomfass, Phys. Rev. **D66**, 045032 (2002); **D63**, 025021 (2001).
 - [13] M. Zapotocky and W.J. Zakrzewski, Phys. Rev. **E51**, R5189 (1995).
 - [14] A.D. Rutenberg, W.J. Zakrzewski, and M. Zapotocky, Europhys. Lett. **39**, 49 (1997).
 - [15] Z. Huang and X.-N. Wang, Phys. Rev. **D49**, 4335 (1994).
 - [16] F. Cooper, Y. Kluger, E.Mottola, and J.P. Paz, Phys. Rev. **D51**, 2377 (1995).
 - [17] M.A. Lampert, J.F. Dawson, and F. Cooper, Phys. Rev. **D54**, 2213 (1996).
 - [18] J. Randrup, Phys. Rev. Lett. **77**, 1226 (1996).
 - [19] J. Randrup, Nucl. Phys. **A616**, 531 (1997).
 - [20] T.C. Petersen and J. Randrup, Phys. Rev. **C61**, 024906 (2000).
 - [21] O. Scavenius, A. Dumitru, and A.D. Jackson, Phys. Rev. Lett. **87**, 182302 (2001).
 - [22] R. Rajaraman: *Solitons and Instantons*, North Holland Publ. Comp., Amsterdam 1982